EBioMedicine 11 (2016) 165–172

Contents lists available at ScienceDirect

EBioMedicine

journal homepage: www.ebiomedicine.com

Research Paper

Laser Therapy Inhibits Tumor Growth in Mice by Promoting Immune Surveillance and Vessel Normalization

Giulia Ottaviani [a,b], Valentina Martinelli [b], Katia Rupel [a,b], Nicoletta Caronni [d], Asma Naseem [d], Lorenzo Zandonà [c], Giuseppe Perinetti [a], Margherita Gobbo [a], Roberto Di Lenarda [a], Rossana Bussani [c], Federica Benvenuti [d], Mauro Giacca [c,e], Matteo Biasotto [a], Serena Zacchigna [b,c,*]

[a] Division of Oral Medicine and Pathology, University Hospital of Trieste, Piazza dell'Ospitale 1, 34129 Trieste, Italy
[b] Cardiovascular Biology, International Centre for Genetic Engineering and Biotechnology (ICGEB), Padriciano 99, 34149 Trieste, Italy
[c] Department of Medical, Surgical and Health Sciences, University Hospital of Trieste, Strada di Fiume, 447, 34149 Trieste, Italy
[d] Cellular Immunology, International Centre for Genetic Engineering and Biotechnology (ICGEB), Padriciano 99, 34149 Trieste, Italy
[e] Molecular Medicine, International Centre for Genetic Engineering and Biotechnology (ICGEB), Padriciano 99, 34149 Trieste, Italy

ARTICLE INFO

Article history:
Received 2 May 2016
Received in revised form 21 July 2016
Accepted 22 July 2016
Available online 25 July 2016

ABSTRACT

Laser therapy, recently renamed as photobiomodulation, stands as a promising supportive treatment for oral mucositis induced by oncological therapies. However, its mechanisms of action and, more importantly, its safety in cancer patients, are still unclear. Here we explored the anti-cancer effect of 3 laser protocols, set at the most commonly used wavelengths, in B16F10 melanoma and oral carcinogenesis mouse models. While laser light increased cell metabolism in cultured cells, the in vivo outcome was reduced tumor progression. This striking, unexpected result, was paralleled by the recruitment of immune cells, in particular T lymphocytes and dendritic cells, which secreted type I interferons. Laser light also reduced the number of highly angiogenic macrophages within the tumor mass and promoted vessel normalization, an emerging strategy to control tumor progression. Collectively, these results set photobiomodulation as a safety procedure in oncological patients and open the way to its innovative use for cancer therapy.

1. Introduction

The number of clinical and preclinical studies, assessing the use of laser light in the prevention and treatment of oral mucositis (OM) in oncological patients undergoing chemo and/or radiotherapy, is rapidly growing (Migliorati et al., 2013). Despite the exact mechanisms by which laser light impacts on biological tissues have not been clarified, the remarkable reduction in local inflammation and promotion of wound healing (Lins et al., 2010), eventually results in a rapid analgesic effect and in a net improvement in the quality of life of the patients (Chung et al., 2012).

Since 2009, we are successfully exploiting Class IV laser light in our clinical practice for both the prevention and the treatment of radio/chemo-induced OM and dermatitis (Chermetz et al., 2014, GOBBO et al., 2014, Ottaviani et al., 2013, Gobbo et al., 2016), constantly obtaining a faster wound healing and a reduced relapse frequency. We have recently compared the efficacy of low-power and high-power laser therapy (LPLT and HPLT) approaches, differing in their wavelength (635 nm for the LPLT and 970 nm for the HPLT) and thus in tissue penetration capacity. We found that both protocols, but mostly HPLT, are able to stimulate the formation of new arterial vessels and the proliferation of vascular smooth muscle cells (Ottaviani et al., 2013).

These encouraging results also opened additional, relevant questions. In particular, considering that the laser therapy, recently named as photobiomodulation (PBM) (Anders et al., 2015), is often applied to head and neck oncological patients, what could be the consequence of promoting angiogenesis and cell proliferation on either dysplastic or neoplastic lesions within the oral cavity of the patients? A few studies have so far assessed the effect of laser light on cancer cell metabolism and proliferation, supporting the hypothesis that PBM could foster the development and the growth of neoplastic lesions (De Castro et al., 2005, Sperandio et al., 2013). However, studies investigating the effects of laser irradiation on different tumor cell lines in vitro have generated conflicting results, and very few of them considered the behavior of tumor cells in vivo, using different protocols and obtaining inconsistent data (Frigo et al., 2009).

Based on these considerations, here we explored the effect of PBM both in cultured cells and in various in vivo models of cancer. In

* Corresponding author at: Cardiovascular Biology, International Centre for Genetic Engineering and Biotechnology (ICGEB), Padriciano 99, 34149 Trieste, Italy.
E-mail address: zacchign@icgeb.org (S. Zacchigna).

http://dx.doi.org/10.1016/j.ebiom.2016.07.028

particular, we compared the activity of 3 different laser protocols (L1, L2 and L3), based on the wavelengths most commonly used in pre-clinical and clinical studies (660, 800 and 970 nm, respectively).

2. Material and Methods

2.1. Laser Devices and Protocols

A gallium arsenide (GaAs) + indium gallium aluminium arsenide phosphide (InGaAlAsP) diode laser device (class IV, K-Laser Cube series, K-laser d.o.o., Sežana, Slovenia) was employed to irradiate cultured cells and animals. To provide a uniform irradiation to multiwell plates, the device was equipped with an adapted prototype probe, specifically designed by Eltech S.r.l. Cells were seeded on sterile 24-well plates (well area: 2 cm^2) in 500 μl of medium without cover during irradiation. The emission tip was hold perpendicular above the culture media and the irradiation was carefully timed and carried out in a dark room. The diode area laser source consisted of equal diodes, which emitted an elliptic laser field with a Gaussian distribution of irradiance (Zacchigna et al., 2014). The emitted light completely covered the irradiated field of each culture plate, as assessed using an optical power meter. The control group was not exposed to laser, but during the laser treatment dishes were removed from the incubator, the cover was removed and cells were kept at room temperature (RT). Three different laser protocols were employed:

- L1: λ 660 nm, laser power 100 mW, irradiance 50 mW/cm^2, fluence 3 J/cm^2, time 60 s, continuous wave
- L2: λ 800 nm, laser power 1 W, irradiance 200 mW/cm^2, fluence 6 J/cm^2, time 30 s, continuous wave
- L3: λ 970 nm, laser power 2.5 W, irradiance 200 mW/cm^2, fluence 6 J/cm^2, time 30 s, continuous wave

The same protocols were applied in vivo, once a day for 4 consecutive days, keeping the laser pointer perpendicular above the affected tissues (tumor area 2 cm^2).

2.2. Cell Lines and Primary Cells

Mouse B16F10 melanoma cells (CRL-6475; ATCC) and human bone osteosarcoma cells (U2OS, HTB-96; ATCC) were grown in complete medium with DMEM 1 g/L glucose supplemented with 10% of FBS, 2 mM L-glutamine, penicillin and streptomycin.

Human skin fibroblasts (HSF, PCS-201-012; ATCC) were plated in complete medium (PCS-201-041; ATCC). Commercial human umbilical vein endothelial cells (HUVEC, CRL-1730; ATCC) were seeded onto gelatin pre-coated acrylic plates, in complete medium (EGM, CC-2517; Lonza). Primary bone marrow-dendritic cells (BM-DCs) were isolated by flushing femura and tibiae of C57BL/6 male mice with RPMI-1640, followed by red blood cell lysis with Ammonium-Chloride-Potassium (ACK) buffer and supplementation with murine recombinant granulocyte macrophage-colony stimulating factor (GM-CSF, 800 U/ml). Aggregates of BM-DCs, evident upon removal of granulocytes and residual lymphocytes, were dislodged by gentle pipetting, counted and plated. mDCs were harvested after 7 days, when the number of $CD11c^+$ was higher than 80%. DCs were also treated with lipopolysaccharide (LPS, 200 ng/ml) endotoxin to promote the secretion of pro-inflammatory cytokine.

2.3. In Vitro ATP Production Assay

Cells plated on 24-well plates were exposed to the various laser protocols and cell proliferation was measured at 24 and 48 h using the ATPlite Luminescence Assay System (PerkinElmer, Waltham, MA), according to manufacturer's instructions. Experiments were performed on 3 biological replicates, each one consisting of 3 technical replicates.

2.4. Animal Models

Animal care and treatment were conducted in conformity with institutional guidelines in compliance with national and international laws and policies (European Economic Community Council Directive 86/609, OJL 358, December 12, 1987) and upon approval by the Institutional Animal Care Use Committee and by the Italian Minister of Health. *Ifnar1*$^{-/-}$ (IFNAR KO) mice, lacking the α chain of the type IFN α/β receptor. on a C57BL/6 background were provided by U. Kalinke (Twincore, Hannover Germany).

Animals (n = 48 C57BL/6 and n = 24, IFNAR KO 6-week-old female mice) were housed under controlled environmental conditions for 5 days with a 12-hour light/dark cycle. Each animal was injected with 1×10^6 B16F10 melanoma cells at the dorsal subcutaneous level. After 10 days, when all masses were clearly detectable, C57BL/6 and IFNAR KO mice were homogenously divided according to tumor size into 4 and 2 groups, respectively. C57BL/6 mice were treated with L1, L2 and L3 protocols, while IFNAR KO mice with L3 protocol from day 11 to 14, whereas one group was used as a control. Tumor volume and mice weight were daily evaluated using a caliper and calculated applying the following formula: $V = \pi/6 * (d^2_{max} * d_{min}/2)$ (Tomayko and Reynolds, 1989). At the end of the experiment (day 15) tumor masses were eventually harvested for accurate measurement of their volume and weight, prior to histological or flow cytometry analysis.

For the oral carcinogenesis model, 50 6-week-old C57BL/6 female mice were used, following the same guidelines described above. The 4-NQO carcinogen (Sigma-Aldrich) was dissolved in propylene glycol (4 mg/ml), diluted in the drinking water to a final concentration of 50 μg/ml, administered to mice for 16 weeks and replaced by regular water starting from the 17th week. All mice were weighed every 4 weeks (Chang et al., 2010, Hawkins et al., 1994). Mice were randomized to receive only the 4-NQO carcinogen (n = 25, control) or to be also exposed to the L3 laser protocol (n = 25, laser group) for 4 consecutive days during the 20th week. Dysplastic and neoplastic oral lesions, mostly located on the ventral side of the tongue, were diagnosed and processed to both macroscopic and microscopic examination by week 21.

The minimal number of animals compatible with obtaining valid scientific results was calculated by a statistical design of the sample size using the software http://homepage.stat.uiowa.edu/~rlenth/Power/, setting a variation coefficient (s) of 30%, alpha of 5%, and a power of 80% (p).

Randomization was performed using a random number schedule and the main experimenter was blind to group assignment.

2.5. Evaluation of Thermal Effect

The temperature of the medium inside the cell culture wells and on the body surface of mice was monitored at baseline, during and after PBM using the Ti20 Thermal Imager (Fluke), as graphically described in Supplementary Fig. S1.

2.6. Histology and Immunofluorescence

For histopathological evaluation, 5 μm tissue sections were stained with haematoxylin and eosin and analyzed by three independent reviewers. The observed lesions were classified into 5 different types: mild dysplasia (D1), moderate dysplasia (D2), severe dysplasia (D3), in situ squamous cell carcinoma (SCC) or invasive SCC. Histopathological diagnosis and grading were based on established criteria (Akhter et al., 2011, Tang et al., 2004) to obtain the following measures: i) the extension of each lesion (D1, D2, D3, in situ SCC, invasive SCC), expressed as a percentage of the total perimeter of the tongue; ii) the

number of areas involved by D1, D2, D3, in situ SCC, invasive SCC on each tongue.

For immunohistochemistry tissue sections were stained with anti-CD4, –CD8 (both from (Abgent), –DCIR2 (Novus Biologicals) and Melan-A (Dako) primary antibodies (1:200), followed by Vectastain ABC kit (Vector Laboratories), according to manufacturer's instructions. For immunofluorescence, tissue sections were stained with fluorescein isothiocyanate-labeled lectin (Lycopersicum esculentum; Vector Laboratories), cyanine 3-labeled anti-αSMA antibodies (Sigma-Aldrich), anti-BrdU (Abcam) or anti-CD31 (Pharmingen Becton Dickinson). All primary antibodies were diluted 1:100, followed by AlexaFluor-conjugated secondary antibodies (Molecular Probes, 1:2000). Image acquisition was performed using either the ImageXpress Micro high-content screening microscope (Molecular Devices) or confocal microscopy (LSM510 META; Carl Zeiss) for subsequent three-dimensional (3D) reconstruction of the vascular network.

2.7. Real Time PCR

Total RNA was extracted using TRIzol (Invitrogen) and reverse transcribed using hexameric random primers (Invitrogen). PCR amplification was performed using TaqMan Gene Expression Assays (AppliedBiosystems). The RPL-37 housekeeping gene was used to normalize the results. Experiments were performed on 3 biological replicates, each one consisting of 3 technical replicates.

2.8. Flow Cytometry

For tumor infiltrate analysis, tumors were harvested 10 days after inoculation, digested with Collagenase type 2 (Worthington-Biochemical Corporation), 265 U/ml for 30 min at 37 °C IV and then smashed through a 70-μm nylon mesh filter (BD Falcon). Part of the mice was subjected to in vivo perfusion with PBS before tumor explantation to remove all blood cells, whereas tumors not subjected to perfusion were treated with Ammonium-Chloride-Potassium (ACK) Lysing Buffer (Gibco-ThermoFisher Scientific) for red blood cell lysis. For surface staining, cells were incubated with anti-Fc receptor antibody (clone 93) and stained with antibodies in PBS + 1% bovine serum albumin for 30 min on ice. Antibodies against CD45 (30-F11), CD11b (M1/70), Ly6C (HK1.4), CD19 (1D3), CD4 (GK1.5) and CD8 (53-6.7) were purchased from Biolegend, against CD11c (N418) and I-A/I-E (M5/114.15.2) were purchased from eBioscience, against *F*4/80 (A13) were purchased from Serotec. Analysis was performed using FACS Aria II (BD Bioscience), according to the gating strategy shown in Supplementary Fig. S2. Dead cells were marked by the LIVE/DEAD Fixable Cell Stain (Invitrogen-ThermoFisher Scientific), which.

permeates the compromised membranes of necrotic cells and reacts with free amines both inside the cells and on the cell surface, resulting in intense fluorescent staining. In contrast, in viable cells only the cell-surface amines are available to react with the dye, resulting in relatively dim staining. Dead cells, corresponding to the brightest population in Supplementary Fig. S2, were excluded from the analysis.

2.9. Statistical analysis

Statistical significance of the differences among the groups within each time point for cell proliferation, and RT-PCR results was assessed by two-way analysis of variance for repeated measurements using the Kruskal–Wallis test.

In the case of experiments entailing the follow-up of the same animals over multiple time points, ANOVA on repeated measures (followed by Bonferroni post-hoc analysis) was used to analyze statistical significance of the differences between groups over time. All the differences concerning mice weight over time within each group were examined using the non-parametric Friedman test.

All statistical assessments were two-sided, and P values <0.05 were considered significant. All analyses were performed using the SPSS 15.0 software.

3. Results

3.1. Laser Treatment Inhibits Tumor Growth and Invasion Without Directly Affecting Tumor Cell Proliferation

To start exploring the possible effect of laser light on cell proliferation, we exposed various primary and cancer cell lines to three laser protocols (L1, L2 and L3), set at increasing wavelengths. All protocols slightly increased ATP content in primary skin fibroblasts at 24 h and this effect was maintained at 48 h especially for the L3 protocol (Supplementary Fig. S3a). In the case of primary endothelial cells, the most effective protocols were L2 and L3 at both time points (Supplementary Fig. S3b). Cell proliferation was transiently increased by laser treatment also in U2OS osteosarcoma cells (L2 and L3 protocols) and B16F10 melanoma cells (L3 protocol), but no significant differences in ATP content or cell counts (not shown) were observed at 48 h after laser irradiation for none of the tested cancer cells (Supplementary Fig. S3c, d). No significant changes in temperature were detected by a Thermal Imager for any of the employed protocols (Supplementary Fig. S1a).

We then investigated the effect of the same protocols on tumor growth in vivo, upon injection of B16F10 cells subcutaneously in syngeneic C57BL/6 mice. All the animals developed a visible tumor mass of comparable size 10 days after cell implantation, when they were randomly divided into 4 experimental groups, each one assigned to a different laser protocol (L1, L2, and L3) or left untreated (control). As shown in Fig. 1a, the volume of the tumor mass progressively increased in all groups, but starting from the last day of laser treatment (day 14), a clear reduction in tumor growth rate was evident for all the three laser protocols ($P < 0.05$ and $P < 0.01$ at day 14 and 15, respectively). No significant differences in either body weight or local body temperature were observed as a consequence of PBM with all the employed protocols over time (Supplementary Figs. S3e and S1b).

Microscopic evaluation of tumor sections upon Melan-A staining, which labels melanoma cells, revealed a remarkable infiltration of tumor cells in the surrounding tissue in control animals (Fig. 1b upper panels and 1c). A clear reduction in the number of infiltrating cells was observed particularly upon tumor irradiation using the L3 protocol (Fig. 1c and b, lower panels).

Thus, while laser light seems to increase the proliferation of cultured cells, the net effect in vivo is a reduction of tumor growth and tumor cell infiltration in surrounding tissues. This effect is mostly evident for the L3 protocol, which displays intermediate light penetration and the highest power density.

3.2. Laser treatment improves perfusion and maturation of tumor vessels

Inspired by this unexpected finding, namely that laser light reduced rather than increasing, tumor growth in vivo and by our previous data supporting the angiogenic effect of PBM, we analyzed the tumor vascular network in treated and untreated animals. While we did not detect any difference in the number of $CD31^+$ endothelial cells, all the three tested protocols markedly increased the number of α-SMA^+ arteries in both the tumoral and peri-tumoral areas (Fig. 1d, e). Considering the importance of tumor-associated macrophages in controlling both tumor growth and vascularization, we quantitatively assess macrophage infiltration by flow cytometry. The analysis was performed either on the whole tumor mass including the intravascular compartment, or upon in vivo perfusion, thus excluding the intravascular compartment. The total number of $F4/80^+$ cells, which most likely tumor associated macrophages, was not significantly modified by laser treatment, either in perfused or not perfused tumors, (Supplementary Fig. S4a) and immunohistochemistry (Supplementary Fig. S4b). Next, we better defined

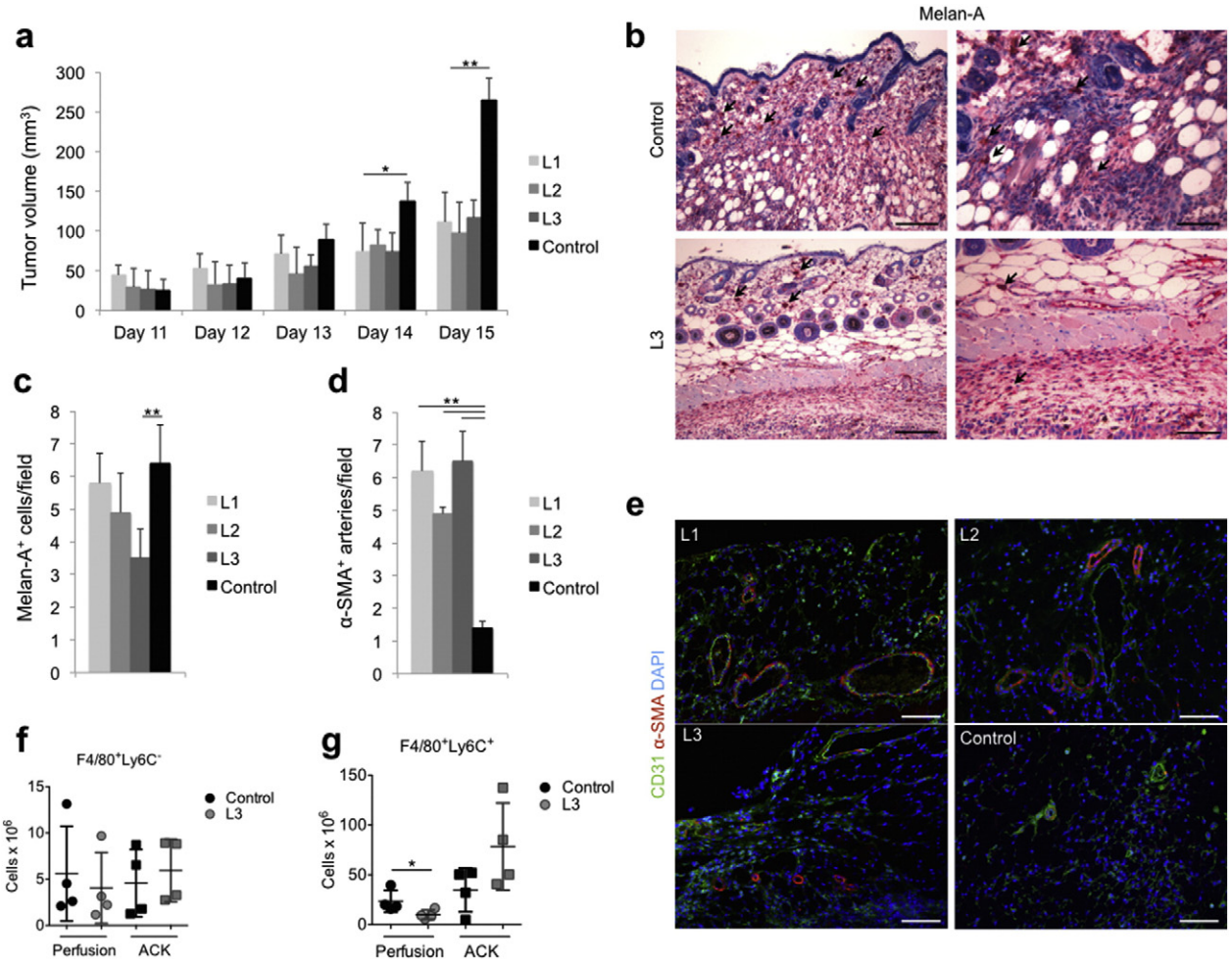

Fig. 1. Laser treatment reduces melanoma growth and invasion while promoting maturation of tumor vessels. a. Assessment of tumor volume upon subcutaneous implantation of B16F10 melanoma cells in C57BL/6 mice. b. Representative pictures of invasive Melan-A$^+$ melanoma cells (black arrows) in the peritumoral area. Scale bar: 100 μm in the left panels and 200 μm in the right panels. c. Number of Melan-A$^+$ melanoma cells/field in the peritumoral area. d. Number of α-SMA$^+$ arteries/field in the peritumoral area. e. Immunofluorescence staining of tumor vasculature showing CD31$^+$ endothelial cells (green), α-SMA$^+$ smooth muscle cells (red). Nuclei are stained with DAPI (blue). Scale bar: 100 μm. f, g. Flow cytometry analysis of F4/80$^+$Ly6C$^-$ (f) and F4/80$^+$Ly6C$^+$ pro-angiogenic macrophages (g), per gram of tumor, upon either in vivo perfusion or red blood cell lysis by Ammonium-Chloride-Potassium (ACK). Data in a, c, d, f and g are expressed as means ± SD, $^*P < 0.05$, $^{**}P < 0.01$.

macrophage phenotype by sub-dividing them according to the relative expression level of the Ly6C antigen. While F4/80$^+$ Ly6C$^-$ macrophages were equally represented in perfused and not perfused tumors, and not even changed upon laser treatment (Fig. 1f), clear differences were detected in the abundance of F4/80$^+$ Ly6C$^+$ macrophages, typically associated to invasive, highly vascularized cancers (Movahedi et al., 2010). Indeed, while these cells tended to be more represented within the intravascular compartment of laser-irradiated tumors, their extravascular content was significantly reduced by laser treatment (Fig. 1g). This capacity of laser light to reduce the number of resident F4/80$^+$ Ly6C$^+$ macrophages, while increasing their intravascular content, is fully compatible with en effect of laser on improving the function of tumor vessels, thereby resulting in increased tumor perfusion. Thus, L3 laser treatment is effective in promoting structural and functional maturation of tumor vessels in the melanoma syngeneic model.

We than validated the effect of laser light on tumor angiogenesis and growth in a model of oral carcinogenesis, which better reproduces the clinical condition. The administration of 4-NQO in the drinking water for 16 weeks resulted in the appearance of either dysplastic or neoplastic lesions in 100% of the animal tongues by week 20, when animals were randomly divided into 2 groups, to be either exposed to the L3 protocol (the most effective protocol in the previous experiments) or left untreated as controls. We first stained tongue sections using anti-CD31 and anti-α-SMA antibodies. While CD31$^+$ capillaries appeared to have a more regular pattern but were not increased in number (not shown), α-SMA$^+$ arterioles were again significantly increased in laser-treated lesions (Fig. 2a, b). We also perfused the animals with fluorescein-labeled lectin to stain the intraluminal side of blood vessels. Whereas control lesions showed an irregular pattern of vessels and extravascular diffusion of the dye, indicating abnormal vascular permeability, laser treatment resulted in a more regular and structured vessel pattern, in the absence of dye leakage (Fig. 2c and Supplementary Movies 1,2). What are the consequences of these vascular changes on cancerogenesis progression? L3 laser treatment reduced the appearance of all kind of dysplastic lesions (D1, D2 and D3; D1 + D2 + D3: 73 in the control and 58 in the L3 groups, respectively; $P < 0.05$) and was even more effective in reducing the number and the percentage of both in situ and invasive carcinomas (total SCC number: 38 in the control and 16 in the L3 groups, respectively; $P < 0.01$; Supplementary Table 1). Of interest, while in the control group, the carcinoma lesions were almost invariably surrounded by waves of dysplastic tissue (essentially D3 and D2 lesions), similar to what normally happens in patients affected by oral SCC, in a few instances the laser treatment resulted in a neoplastic area completely surrounded by healthy tissue, as shown in Fig. 2d.

Thus, laser treatment inhibits tumor progression and improves functional vessel maturation also in a model of oral carcinogenesis.

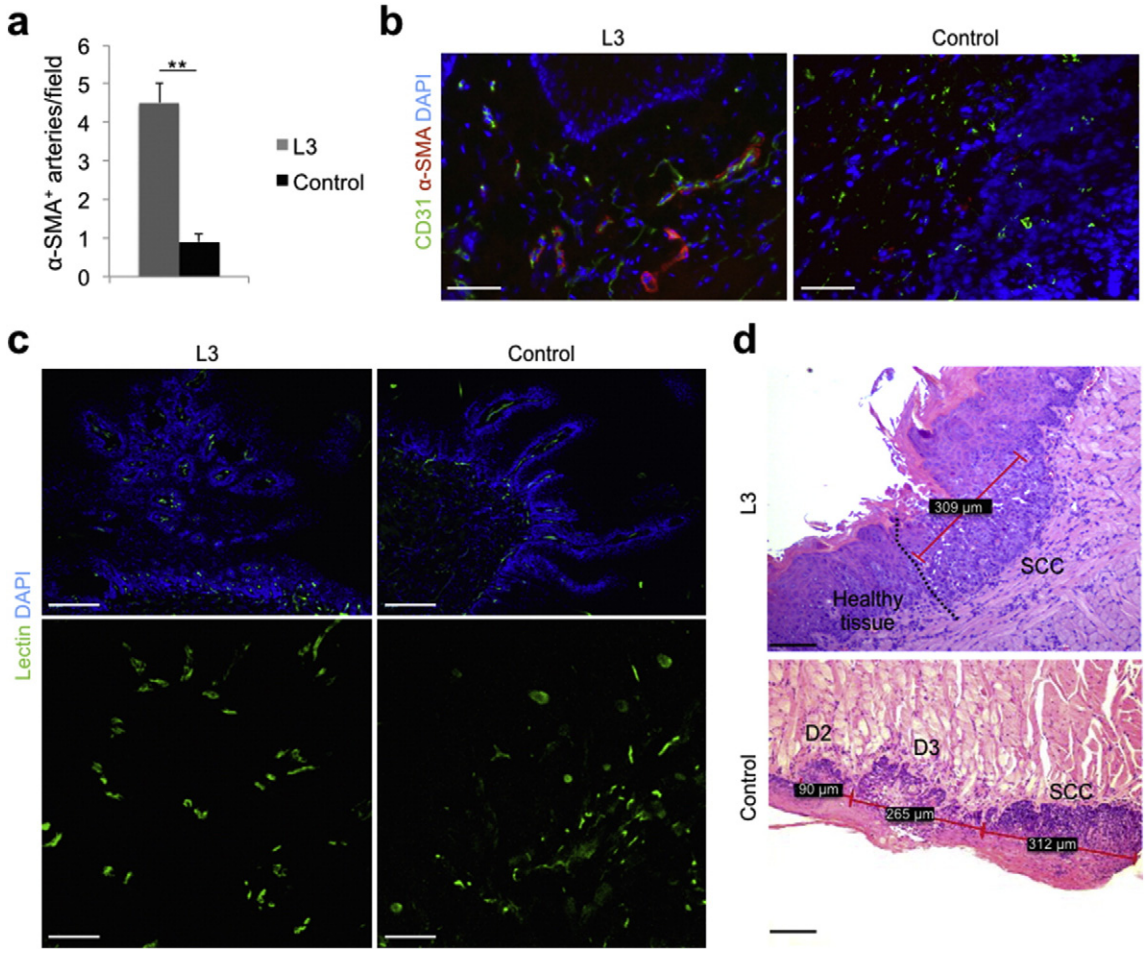

Fig. 2. Laser treatment inhibits tumor growth in a mouse model of oral carcinogenesis. a. Number of α-SMA$^+$ arteries/field in the peritumoral area. Data are expressed as means ± SD; $^{**}P < 0.01$ versus control. b. Immunofluorescence staining of tumor vasculature showing CD31$^+$ endothelial cells (green), α-SMA$^+$ smooth muscle cells (red). Nuclei are stained with DAPI (blue). Scale bar: 50 μm. c. Images of tongue sections from animals perfused in vivo with fluorescein-labeled lectin (green) to stain the intraluminal side of vessels. Nuclei are stained with DAPI (blue). Scale bars: 1 mm (upper panels) and 100 μm (lower panels). d. Haematoxylin-eosin staining of dysplastic and neoplastic lesions arose on mouse tongues upon exposure to 4-NQO. A dividing line can be drawn to separate invasive carcinoma from healthy mucosa in a representative L3-treated animal (upper panel), whereas a wave of progressive dysplasia was always present close to any carcinoma in control group (lower panel). SCC: squamous cell carcinoma. D2: moderate dysplasia. D3: severe dysplasia. Red lines and numbers in the black square box indicate the size of each lesion. Scale bar: 100 μm.

3.3. Laser treatment promotes immune cell recruitment around tumor masses

Based on the evidence that laser light does not directly reduce tumor cell proliferation but rather affected tumor vascularization, partially modulating the infiltration of pro-angiogenic macrophages, we extended the analysis to other immune cell subsets, potentially able to influence tumor microenvironment. We first evaluated the global presence of immune cells using the pan-leukocytic marker CD45. Remarkably, the number of immune cells upon laser irradiation was significantly increased, an increment that was completely lost upon perfusion, indicating that leukocytes mostly resided within the intravascular compartment (Supplementary Fig. S4c) and supporting the effect of laser light in boosting tumor perfusion. We then moved assessing the presence of tumor-infiltrating T lymphocytes (both CD4$^+$ and CD8$^+$ cells), which represent a longstanding topic of interest for their prognostic significance in the outcome of various cancers. By immunohistochemical analysis of the border region between tumor and the surrounding, healthy tissue, we could detect a higher density of these cells (both CD4$^+$ and CD8$^+$ cells), which tended to get closer and unwrap the tumor mass, particularly in the case of the L3 protocol compared to untreated tumors (Fig. 3a and Supplementary Fig. S4d). However, when quantitatively assessing cell infiltration by flow cytometry, we found no significant differences in the content of any T lymphocyte type either in perfused or in not perfused animals (Fig. 3b, c). Similar results were obtained for CD19$^+$ B lymphocytes (Fig. 3d) and CD11b$^+$ Ly6C^{int}F4/80$^-$ SSC^{high} polymorphonuclear neutrophils (PMNs) (Supplementary Fig. S4e), which were equally represented in treated and untreated tumors, regardless of perfusion. Thus, laser light does not have an impact on the number of infiltrating T lymphocytes, but rather causes a re-distribution of these cells around the tumor mass.

Next, we focused our attention on dendritic cells (DCs), which also potently influence tumor growth and invasion. Similar to what we have observed for T lymphocytes, while in control tumors a few DCIR2$^+$ DCs were detected around the neoplastic field, upon laser treatment, and especially upon L2 and L3 protocols, these cells get closer to the tumor cells and often invaded the tumor mass itself (Fig. 3e). The number of infiltrating CD11c$^+$ MHC-II^{high}F4/80$^-$ DCs was not significantly affected by laser treatment neither in perfused nor in not perfused tumors. However, we observed a trend toward increased DC density in L3-treated tumors in not perfused animals (Fig. 3f), suggesting that incoming DCs gather closer to the tumor mass upon treatment.

To better investigate a potential, direct activity of PBM on DCs, we prepared primary DC cultures from the mouse bone marrow. We were

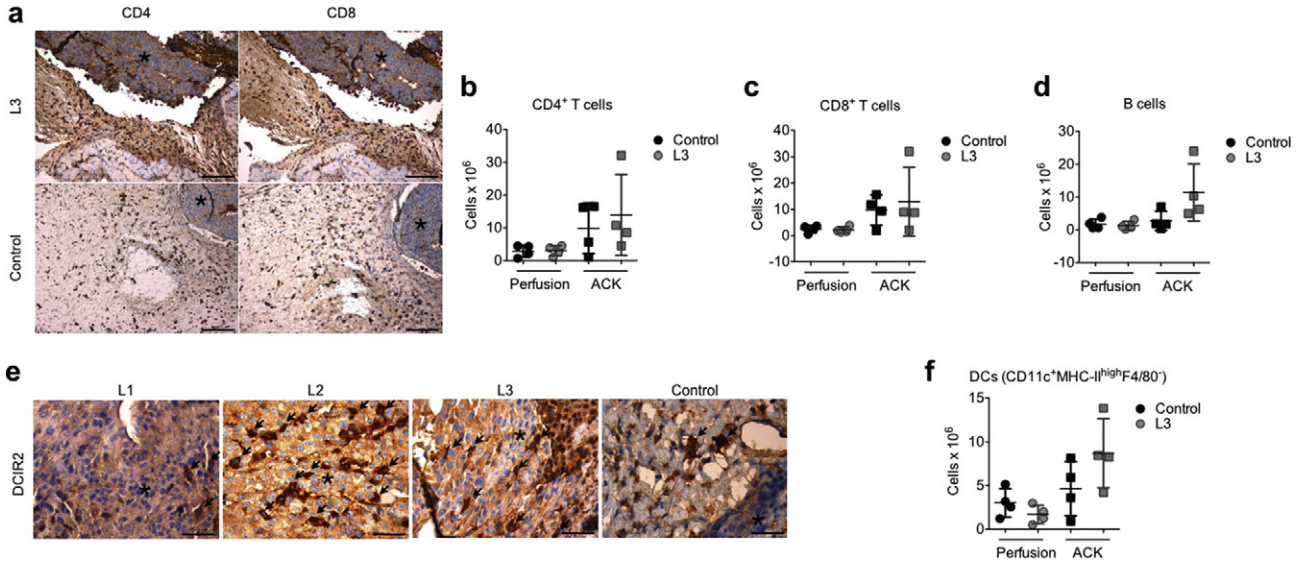

Fig. 3. Laser treatment recruits immune cells around tumor masses. A. Immunohistochemistry of $CD4^+$ and $CD8^+$ lymphocytes inside the B16F10 tumor mass, marked by an asterisk, and in the peri-tumoral area, in control and L3 treated group. Scale bar: 50 μm. b–d and f. Flow cytometry analysis of the number of $CD4^+$ T lymphocytes (b), $CD8^+$ T lymphocytes (c), $CD19^+$ B lymphocytes (d) and $CD11c^+MHC\text{-}II^{high}F4/80^-$ DCs (f) in tumors subjected either to in vivo perfusion or to red blood cell lysis by Ammonium-Chloride-Potassium (ACK). Data are expressed as means ± SD per gram of tumor (no significant differences). e. Immunohistochemistry of $DCIR2^+$ DCs (black arrows) inside the B16F10 tumor mass (black asterisk) in control and laser-treated groups. Scale bar: 100 μm.

not able to detect any increase in cell metabolism/proliferation after exposure of DCs to laser light, either in the presence or in the absence of LPS, a potent inducer of DC activation (Supplementary Fig. S3f). Of interest, when we assessed the capacity of DCs to secrete type I IFNs by ELISA, we observed that the 3 laser protocols remarkably increased the production of these cytokines, and in particular of IFNα, well known for their potent anti-cancer activity (Lim et al., 2014; Picaud et al., 2002) (Fig. 4a). We finally evaluated whether the expression levels of type I IFNs were also changed within melanoma tumors in vivo upon laser treatment and found that the three protocols effectively up-regulated the expression of these cytokines, consistent with their anti-tumor effect (Fig. 4b). Based on these results, we evaluated the effect of L3 laser irradiation on B16F10 tumor growth in IFNα receptor (IFNAR) knockout (KO) mice, characterized by the complete absence of IFNα/β activity (Muller et al., 1994). Tumor development was enhanced in the IFNAR KO animals but not affected by laser treatment at any time point (Fig. 4c). Different from wild type animals, at microscopic evaluation we could not detect any particular recruitment of T lymphocytes,

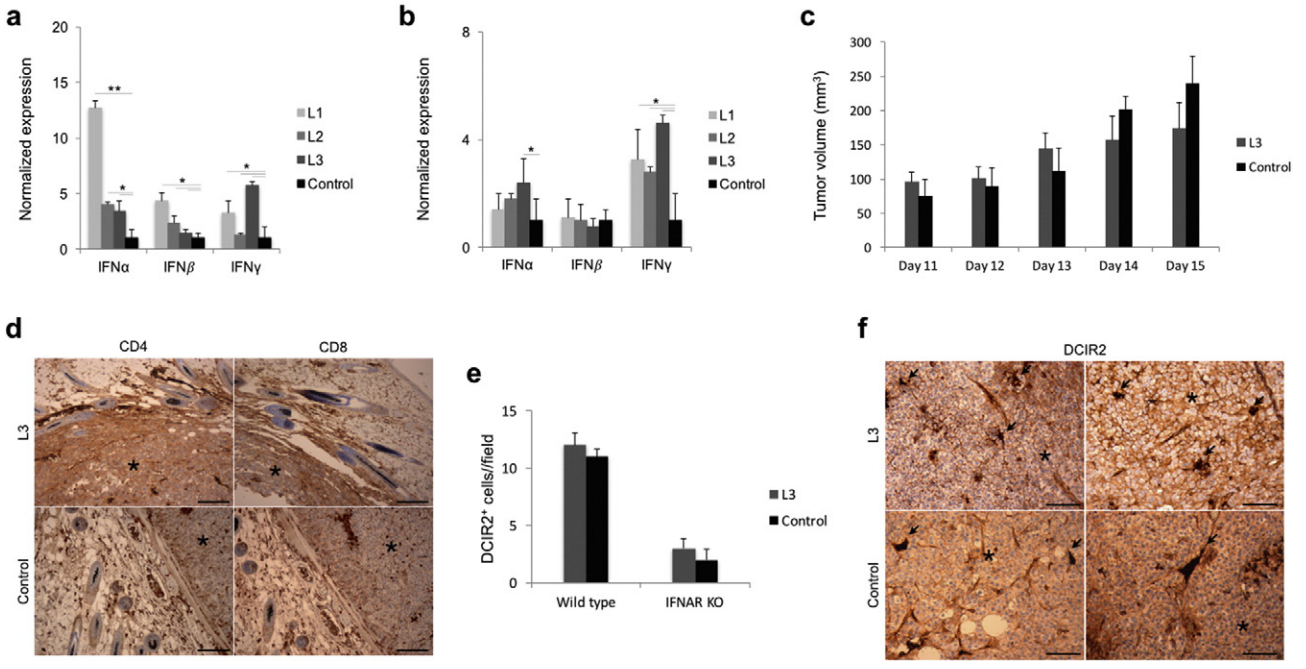

Fig. 4. Effect of laser treatment on DC activation and type I IFNs secretion. a. Real-time quantification of IFNα, IFNβ and IFNγ secreted by primary DCs following laser irradiation (24 h). b. Real-time quantification of IFNα, IFNβ and IFNγ mRNAs from B16F10 melanoma tumors following laser irradiation (day 15). c. Assessment of tumor volume upon subcutaneous implantation of B16F10 melanoma cells in IFNAR KO mice. d. Immunohistochemistry of $CD4^+$ and $CD8^+$ lymphocytes inside the B16F10 tumor mass (marked by an asterisk) and in the peri-tumoral area in control and L3-treated IFNAR KO mice. Scale bar: 50 μm. e. Number of $DCIR2^+$ cells/field in the peritumoral area of wild type and IFNAR KO mice. Data are expressed as means ± SD. f. Immunohistochemistry of $DCIR2^+$ DCs (black arrows) inside the B16F10 tumor mass (black asterisk) in control and L3-treated IFNAR KO mice. Scale bar: 100 μm.

either $CD4^+$ or $CD8^+$ cells, around the tumor mass upon laser treatment (Fig. 4d). The number of DCs surrounding the tumor mass was overall reduced in IFNAR KO animals, but again not affected by laser light (Fig. 4e, f). Thus, laser treatment loses its potential to inhibit tumor growth and to foster immune cell recruitment toward the tumor mass in IFNAR KO mice, indicating a relevant role of IFNα and IFNβ in mediating the effects of laser light in vivo.

4. Discussion

While we have designed this study to assess the safety of PBM, our results provided novel, unexpected results. Not only tumor growth was not increased by laser light, but also the 3 tested protocols effectively reduced lesion size and markedly affected tumor microenvironment in both B16F10 and oral carcinogenesis models. Our study presents the following novelty features: i) it demonstrates that the effect of laser light on cancer cell growth is different in cell culture and in vivo; ii) it shows a remarkable effect of PBM on tumor vasculature, resulting in a more structured and functional vascular network; iii) it unveils a potent activity of laser light on immune modulation and DC activation, mediated by type 1 IFNs.

The need to clearly establish the effect of laser light on cancer stems from our routinely use of this technique for the treatment of radio/chemo-therapy side effects (Chermetz et al., 2014, Gobbo et al., 2014, Ottaviani et al., 2013). Despite a common consensus by the scientific community on the efficacy of PBM on mucosal injuries (Migliorati et al., 2013), very few studies reliably assessed the effects of exposing dysplastic or even cancer tissues to laser irradiation, which represents a realistic scenario in most oncological patients, as residual tumor cells may still be present following oncological treatments for head and neck cancer, even in the absence of macroscopic lesions (Schartinger et al., 2012).

While most of the previous studies mainly assessed the effect of laser light on cancer cells in culture, here we intentionally explored whether PBM exerted the same activity ex vivo and in vivo. We exposed various primary cells and cancer cell lines to different laser protocols (L1, L2 and L3) and noticed that in most instances, the net effect was a significant increase in cell metabolism and proliferation, in agreement with available literature data (Frigo et al., 2009). Of notice, not all cell types responded in the same manner to each protocol, possibly indicating a different content of endogenous porphyrins and cytochromes, which are generally acclaimed as the primary laser light receptors (Farivar et al., 2014). Indeed, primary cells tended to respond better to PBM than cancer cells, which often carry abnormalities in their mitochondria. Most relevant, when irradiating the same B16F10 cells ex vivo and in vivo, we observed an opposite effect. Despite a modest, but significant increase in ATP content was detected in cultured cells upon exposure to the L3, all 3 protocols markedly reduced tumor growth in vivo, as well as the number of neoplastic cells infiltrating and invading of surrounding tissues. These results are consistent with a few published reports assessing the in vivo behavior of tumors exposed to laser light, and showing that low power and energy doses have no influence on tumor growth, or rather they can inhibit it (Abe et al., 1993).

The lower index of tumor growth and invasiveness in laser treated animals, and especially in the L3 group, was accompanied by a notable presence of immune cells (essentially T lymphocytes and DCs) around the tumor mass. These findings are in line with the recent observation that laser light can be exploited to activate dermal DCs to effectively migrate to draining lymph nodes and to induce antigen-specific $CD8^+$ and $CD4^+$ T cell responses in the same melanoma mouse model (Terhorst et al., 2015). Besides opening the way to completely novel strategies to enhance cancer immunotherapy and vaccination in general, these data also shed some light on the mechanisms by which PBM could inhibit tumor growth in vivo, and thus be considered a safe procedure in cancer patients. Notably, we showed that the direct irradiation of primary DCs significantly increased the secretion of type I IFNs and a consistent up-regulation of these cytokines was detected in vivo in B16F10 tumors upon exposure to any of the 3 tested laser protocols. Type I IFNs are well known for their peculiar anti-proliferative, pro-apoptotic and anti-angiogenic properties, which are essential for immunosurveillance of cancer, and already exploited clinically in a variety of malignancies (reviewed in Zitvogel et al., 2015). The observation that laser treatment completely lost its effect in IFNAR KO mice is a clear indication that IFNα and IFNβ are essential mediators of the anti-cancer activity of laser light in vivo. At what extent the activation of immune cells, and in particularly DCs, might also be responsible of the clearance od dysplastic lesions observed in the oral carcinogenesis model, similarly to what observed in human oral SCC (Upadhyay et al., 2012), still remains an open question. Since it is known that mild hyperthermia can exert immune-modulatory activities (Knippertz et al., 2011), we cannot formally exclude that the observed effects derive, at least in part, from cell and tissue heating. However, the evidence that the most effective protocol (L3) did not increase the temperature of either cultured cells or body surface, points toward a minimal, if not null contribution of hyperthermia to the anti-cancer effect of PBM.

From our analysis of intra-tumoral immune cell content by flow cytometry, we invariably detected an increased number of cells in not perfused compared to perfused animals in the L3 group. This is an indirect, albeit strong indication that laser treatment enhanced the perfusion of the tumor mass, thus increasing the number of cells within its intravascular compartment. Of notice, whereas most of the immune cell types were equally abundant within the extravascular space in control and laser-treated animals, L3 therapy resulted in a significant reduction on the number of $F4/80^+Ly6C^+$ cells, which most probably represent pro-angiogenic macrophages. This observation led us to analyze the tumor vasculature in both the B16F10 and the oral carcinogenesis models. In both cases, we observed that laser irradiation resulted in a significant increase in the number of α-SMA^+ arterial vessels and a more regular and structured vessel pattern, as assessed by immunofluorescence and in vivo perfusion with fluorescent lectin. The ultimate outcome of these effects was the reduction of tumor progression, fitting the concept of "vessel normalization", originally put forward as a goal to improve blood supply and enhance drug delivery by low-dose anti-angiogenic agents and more recently emerging as an innovative strategy to inhibit tumor growth rate (Carrer et al., 2012).

Collectively, our results clearly indicate that any experiment assessing the effect of laser light on cultured cells is not representative of the in vivo condition. Indeed, whereas laser light increased cell metabolism and proliferation in cell culture, the overall effect in vivo was a reduced tumor progression. These results were totally unexpected and are definitely exciting in terms of clinical translatability, as they set PBM as a safe procedure and warrant further investigation exploring its inclusion in multimodal anti-cancer protocols in humans. Which protocols should be put forward as the most effective ones? Our data tend to indicate that L1 and L3, set at 660 nm and 970 nm respectively, could be more efficacious than L2 (800 nm) in activating immune cells and normalizing tumor vessels, possibly because of their lower penetration and enhanced activity on the more superficial dermal and sub-mucosal layers, where most of the immune cells and blood vessels normally reside.

Supplementary data to this article can be found online at http://dx.doi.org/10.1016/j.ebiom.2016.07.028.

Funding Sources

Associazione Italiana per la Ricerca sul Cancro (AIRC, MFAG n. 9233) to S. Zacchigna and Italian Ministry of Education, University and Research (MIUR), FIERCE project n. RBAP11Z4Z9 to M. Giacca.

Conflict of Interest Statement

The authors do not have any conflict of interest.

Author Contributions

Conceptualization: S.Z.; Methodology: S.Z. and G.O.; Formal Analysis: G.P.; Investigation: G.O., V.M., K.R., N.C., A.N.; Resources: M.B., R.B., M.G. and L.Z; Writing: S.Z. and G.O.; Visualization: S.Z.; Supervision: S.Z., R.D., F.B. M.G.; Funding Acquisition: S.Z and M.G.

Acknowledgements

We are grateful to S. Artico, W. De Mattia and B. Boziglav for excellent technical support.

References

Abe, M., Fujisawa, K., Suzuki, H., Sugimoto, T., Kanno, T., 1993. Role of 830 nm low reactive level laser on the growth of an implanted glioma in mice. Keio J. Med. 42, 177–179.
Akhter, M., Hossain, S., Rahman, Q.B., Molla, M.R., 2011. A study on histological grading of oral squamous cell carcinoma and its co-relationship with regional metastasis. J. Oral Maxillofac. Pathol. 15, 168–176.
Anders, J.J., Lanzafame, R.J., Arany, P.R., 2015. Low-level light/laser therapy versus photobiomodulation therapy. Photomed. Laser Surg. 33, 183–184.
Carrer, A., Moimas, S., Zacchigna, S., Pattarini, L., Zentilin, L., Ruozi, G., Mano, M., Sinigaglia, M., Maione, F., Serini, G., Giraudo, E., Bussolino, F., Giacca, M., 2012. Neuropilin-1 identifies a subset of bone marrow Gr1- monocytes that can induce tumor vessel normalization and inhibit tumor growth. Cancer Res. 72, 6371–6381.
Chang, N.W., Pei, R.J., Tseng, H.C., Yeh, K.T., Chan, H.C., Lee, M.R., Lin, C., Hsieh, W.T., Kao, M.C., Tsai, M.H., Lin, C.F., 2010. Co-treating with arecoline and 4-nitroquinoline 1-oxide to establish a mouse model mimicking oral tumorigenesis. Chem. Biol. Interact. 183, 231–237.
Chermetz, M., Gobbo, M., Ronfani, L., Ottaviani, G., Zanazzo, G.A., Verzegnassi, F., Treister, N.S., Di Lenarda, R., Biasotto, M., Zacchigna, S., 2014. Class IV laser therapy as treatment for chemotherapy-induced oral mucositis in onco-haematological paediatric patients: a prospective study. Int. J. Paediatr. Dent. 24, 441–449.
Chung, H., Dai, T., Sharma, S.K., Huang, Y.Y., Carroll, J.D., Hamblin, M.R., 2012. The nuts and bolts of low-level laser (light) therapy. Ann. Biomed. Eng. 40, 516–533.
De Castro, J.L., Pinheiro, A.L., Werneck, C.E., Soares, C.P., 2005. The effect of laser therapy on the proliferation of oral KB carcinoma cells: an in vitro study. Photomed. Laser Surg. 23, 586–589.
Farivar, S., Malekshahabi, T., Shiari, R., 2014. Biological effects of low level laser therapy. J. Lasers Med. Sci. 5, 58–62.
Frigo, L., Luppi, J.S., Favero, G.M., Maria, D.A., Penna, S.C., Bjordal, J.M., Bensadoun, R.J., Lopes-Martins, R.A., 2009. The effect of low-level laser irradiation (In-Ga-Al-AsP - 660 nm) on melanoma in vitro and in vivo. BMC Cancer 9, 404.
GOBBO, M., OTTAVIANI, G., PERINETTI, G., CIRIELLO, F., BEORCHIA, A., GIACCA, M., DI LENARDA, R., RUPEL, K., TIRELLI, G., ZACCHIGNA, S., BIASOTTO, M., 2014. Evaluation of nutritional status in head and neck radio-treated patients affected by oral mucositis: efficacy of class IV laser therapy. Support Care Cancer 22, 1851–1856.
Gobbo, M., Ottaviani, G., Rupel, K., Ciriello, F., Beorchia, A., Di Lenarda, R., Zacchigna, S., Biasotto, M., 2016. Same strategy for pitfalls of radiotherapy in different anatomical districts. Lasers Med. Sci.
Hawkins, B.L., Heniford, B.W., Ackermann, D.M., Leonberger, M., Martinez, S.A., Hendler, F.J., 1994. 4NQO carcinogenesis: a mouse model of oral cavity squamous cell carcinoma. Head Neck 16, 424–432.
Knippertz, I., Stein, M.F., Dorrie, J., Schaft, N., Muller, I., Deinzer, A., Steinkasserer, A., Nettelbeck, D.M., 2011. Mild hyperthermia enhances human monocyte-derived dendritic cell functions and offers potential for applications in vaccination strategies. Int. J. Hyperth. 27, 591–603.
Lim, J.Y., Gerber, S.A., Murphy, S.P., Lord, E.M., 2014. Type I interferons induced by radiation therapy mediate recruitment and effector function of CD8(+) T cells. Cancer Immunol. Immunother. 63, 259–271.
Lins, R.D., Dantas, E.M., Lucena, K.C., Catao, M.H., Granville-Garcia, A.F., Carvalho Neto, L.G., 2010. Biostimulation effects of low-power laser in the repair process. An. Bras. Dermatol. 85, 849–855.
Migliorati, C., Hewson, I., Lalla, R.V., Antunes, H.S., Estilo, C.L., Hodgson, B., Lopes, N.N., Schubert, M.M., Bowen, J., Elad, S., Mucositis Study Group of the Multinational Association of Supportive Care in Cancer/International Society of Oral, O, 2013. Systematic review of laser and other light therapy for the management of oral mucositis in cancer patients. Support Care Cancer 21, 333–341.
Movahedi, K., Laoui, D., Gysemans, C., Baeten, M., Stange, G., van den Bossche, J., Mack, M., Pipeleers, D., In't Veld, P., De Baetselier, P., van Ginderachter, J.A., 2010. Different tumor microenvironments contain functionally distinct subsets of macrophages derived from Ly6C(high) monocytes. Cancer Res. 70, 5728–5739.
Muller, U., Steinhoff, U., Reis, L.F., Hemmi, S., Pavlovic, J., Zinkernagel, R.M., Aguet, M., 1994. Functional role of type I and type II interferons in antiviral defense. Science 264, 1918–1921.
Ottaviani, G., Gobbo, M., Sturnega, M., Martinelli, V., Mano, M., Zanconati, F., Bussani, R., Perinetti, G., Long, C.S., Di Lenarda, R., Giacca, M., Biasotto, M., Zacchigna, S., 2013. Effect of class IV laser therapy on chemotherapy-induced oral mucositis: a clinical and experimental study. Am. J. Pathol. 183, 1747–1757.
Picaud, S., Bardot, B., De Maeyer, E., Seif, I., 2002. Enhanced tumor development in mice lacking a functional type I interferon receptor. J. Interf. Cytokine Res. 22, 457–462.
Schartinger, V.H., Galvan, O., Riechelmann, H., Dudas, J., 2012. Differential responses of fibroblasts, non-neoplastic epithelial cells, and oral carcinoma cells to low-level laser therapy. Support Care Cancer 20, 523–529.
Sperandio, F.F., Giudice, F.S., Correa, L., Pinto, D.S., Jr. Hamblin, M.R., De Sousa, S.C., 2013. Low-level laser therapy can produce increased aggressiveness of dysplastic and oral cancer cell lines by modulation of Akt/mTOR signaling pathway. J. Biophotonics 6, 839–847.
Tang, X.H., Knudsen, B., Bemis, D., Tickoo, S., Gudas, L.J., 2004. Oral cavity and esophageal carcinogenesis modeled in carcinogen-treated mice. Clin. Cancer Res. 10, 301–313.
Terhorst, D., Fossum, E., Baranska, A., Tamoutounour, S., Malosse, C., Garbani, M., Braun, R., Lechat, E., Crameri, R., Bogen, B., Henri, S., Malissen, B., 2015. Laser-assisted intradermal delivery of adjuvant-free vaccines targeting XCR1 + dendritic cells induces potent antitumoral responses. J. Immunol. 194, 5895–5902.
Tomayko, M.M., Reynolds, C.P., 1989. Determination of subcutaneous tumor size in athymic (nude) mice. Cancer Chemother. Pharmacol. 24, 148–154.
Upadhyay, J., Rao, N.N., Upadhyay, R.B., 2012. A comparative analysis of langerhans cell in oral epithelial dysplasia and oral squamous cell carcinoma using antibody CD-1a. J. Cancer Res. Ther. 8, 591–597.
Zacchigna, S., Biasotto, M., Zanatta, F., 2014. Authors' reply. Am. J. Pathol. 184, 1251–1252.
Zitvogel, L., Galluzzi, L., Kepp, O., Smyth, M.J., Kroemer, G., 2015. Type I interferons in anticancer immunity. Nat. Rev. Immunol. 15, 405–414.